

Supporting Information

Fabrication of hierarchical mesoporous $MnCo_2O_4$ and $CoMn_2O_4$ microspheres that are composed of polyhedral nanoparticles as promising anodes for long-life LIBs

Guangda Li, Liqiang Xu, Yanjun Zhai and Yaping Hou*

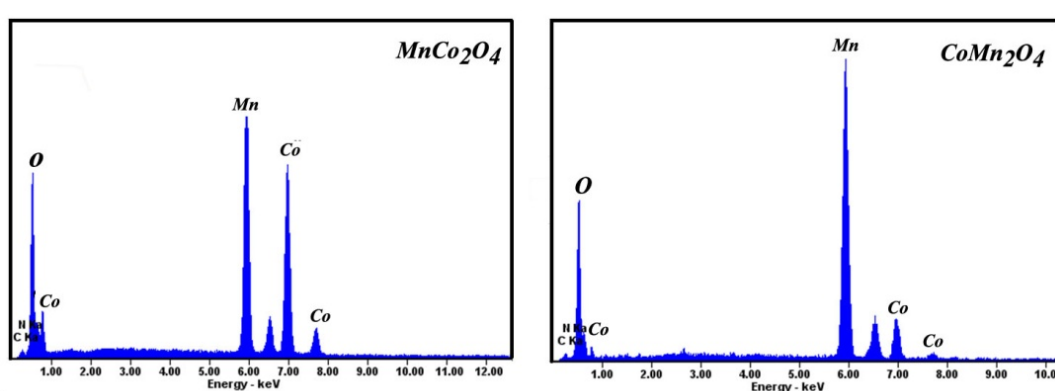


Fig. S1 EDX spectra of the as-obtained $MnCo_2O_4$ and $CoMn_2O_4$.

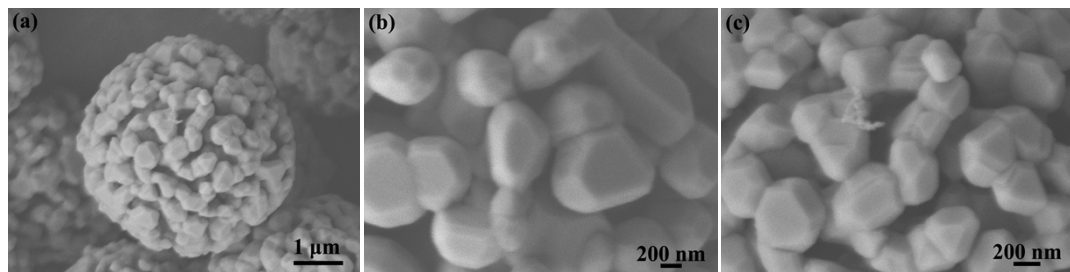


Fig. S2 Magnified SEM images of the porous $MnCo_2O_4$ microsphere.

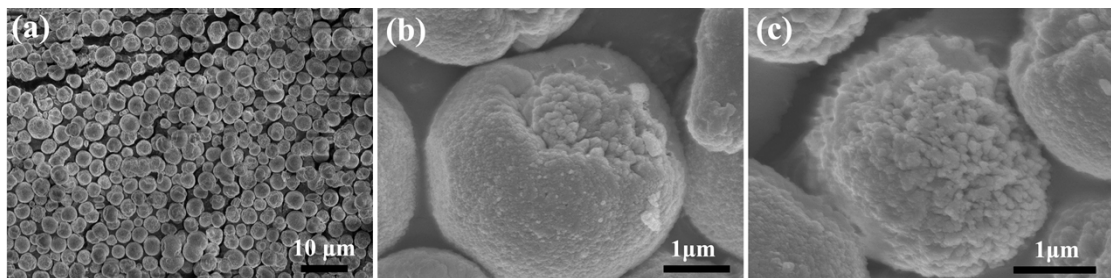


Fig. S3 FESEM images of $\text{Mn}_{0.33}\text{Co}_{0.67}\text{CO}_3$ (MnCo-precursor).

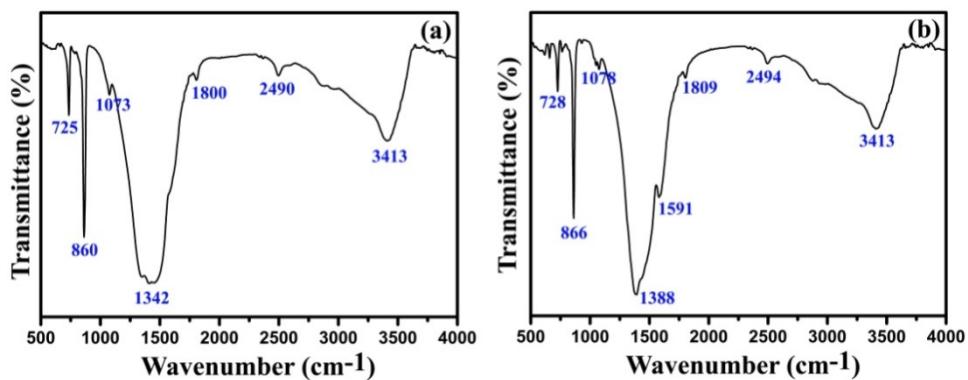


Fig. S4 FTIR spectra of the precursors of (a) $\text{Mn}_{0.33}\text{Co}_{0.67}$ and (b) $\text{Co}_{0.33}\text{Mn}_{0.67}\text{CO}_3$.

The peak centered at 3413cm^{-1} evidences the presence of O-H stretching vibration, indicating a tiny amount of moisture exists in samples. The stretching vibration and the in-plane flexural vibration of the N-H bond are observed at 2490 and 1800 cm^{-1} , respectively, which come from HMT adsorption on the precursors. In addition, the peaks at 1388 , 1073 , 866 , 728 cm^{-1} , a feature of carbonate,^[1-2] can be ascribed to the $\text{Mn}_{0.33}\text{Co}_{0.67}$ and $\text{Co}_{0.33}\text{Mn}_{0.67}\text{CO}_3$ precursors.

[1] P. Huang, X. Zhang, J. M. Wei, J. Q. Pan, Y. Z. Sheng, B. X. Feng, *Mater. Chem. Phys.*, **2014**, *147*, 996.

[2] L. M. Song, S. J. Zhang, X. Q. Wu, Z. L. Wang, Q. W. Wei, *Chem. Eng. J.*, **2012**, *15*, 195.

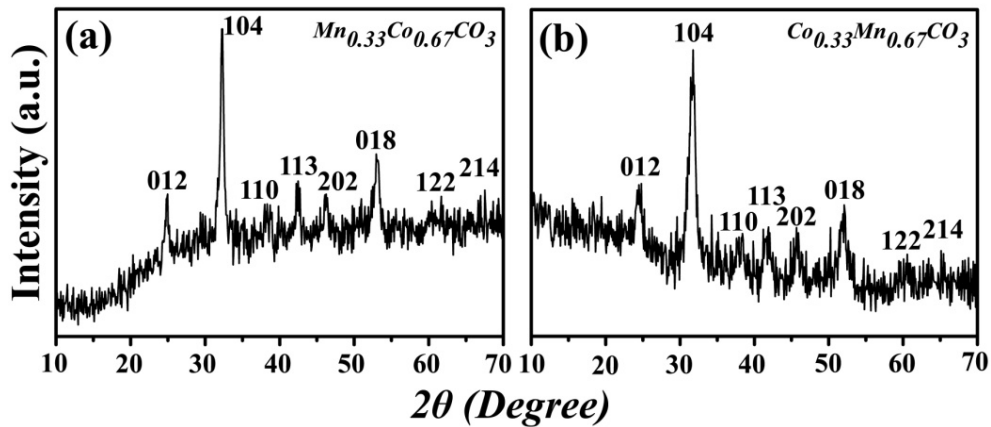


Fig. S5 XRD patterns of the precursors of (a) $Mn_{0.33}Co_{0.67}CO_3$ and (b) $Co_{0.33}Mn_{0.67}CO_3$.

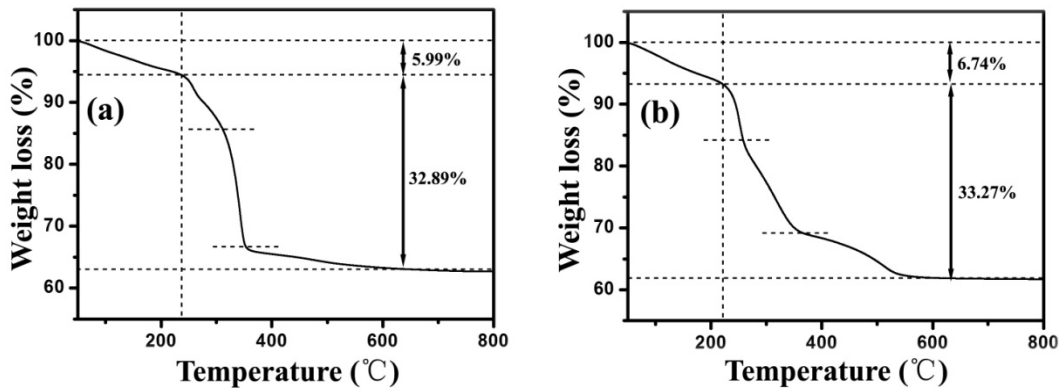


Fig. S6 TGA curves of the (a) $Mn_{0.33}Co_{0.67}CO_3$ and (b) $Co_{0.33}Mn_{0.67}CO_3$ precursors.

In order to investigation of the thermal behavior of $Mn_{0.33}Co_{0.67}CO_3$ and $Co_{0.33}Mn_{0.67}CO_3$ microspheres, TGA curves of the presuesors under atmosphere are shown in Figure S5. The TGA curves could be categorized into two major weight loss processes. The first weight loss below ~ 230 °C is attributed to the loss of physical and chemical adsorption on the surface of precursor particles, such as H_2O , HMT and other organic compounds which produced in solvothermal process. The second conspicuous weight loss is due to the thermal decomposition of precursors into

MnCo_2O_4 and CoMn_2O_4 , and at the same time, released CO_2 with temperature increasing. For $\text{Mn}_{0.33}\text{Co}_{0.67}\text{CO}_3$ and $\text{Co}_{0.33}\text{Mn}_{0.67}\text{CO}_3$ precursors, the value of the second weight are 32.89% and 32.27%, respectively, which are very consistent with the theoretical value (32.87% and 33.23%). TGA, together with XRD and IR, confirmed the ingredient of the precursors perfectly. Furthermore, it was also found that the second major weight loss can be divided into three processed because of the different thermal behaviors of MnCO_3 and CoCO_3 . The similar phenomenon was also observed in previous works.^[1,2] According to the TGA curves, the optimal temperature for obtaining MnCo_2O_4 and CoMn_2O_4 is carried out at 600 °C.

[1] J. F. Li, S. L. Xiong, X. W. Li, Y. T. Qian, *Nanoscale*, **2013**, 5, 2045.

[2] X. F. Chen, L. L. Zhang, W. X. Zhang, Y. H. Huang, *J. Alloy Comp.*, **2013**, 559, 5.

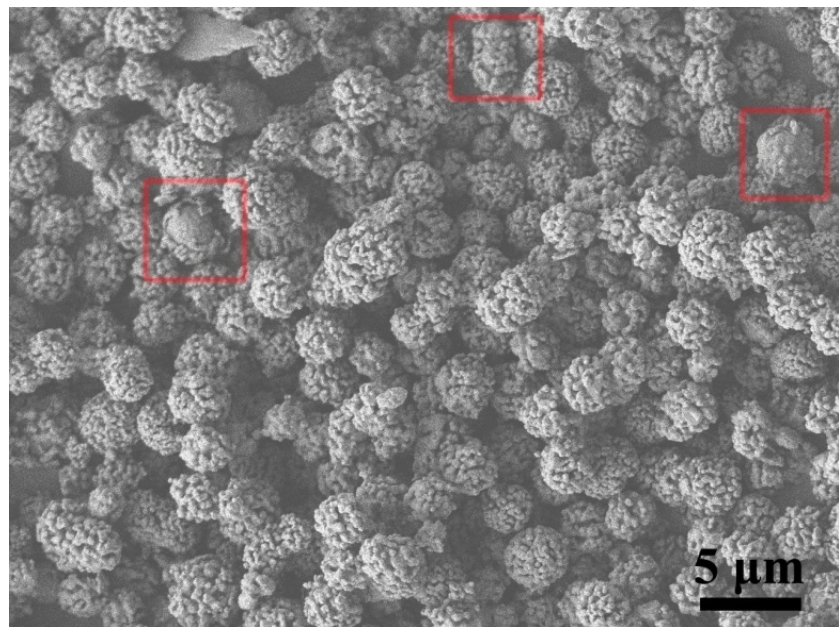


Fig. S7 FESEM image of the $\text{Mn}_{0.33}\text{Co}_{0.67}\text{CO}_3$ after annealed for 4 h at 600 °C.

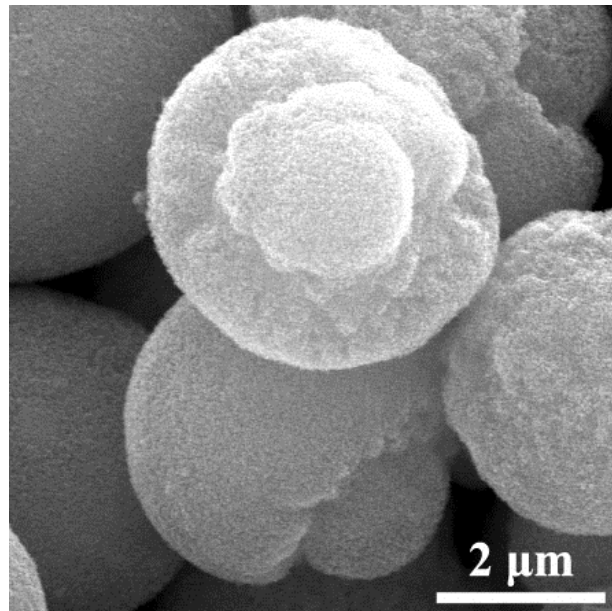


Fig. S8 FESEM image of the broken MnCo_2O_4 microsphere at 600 °C for 6 h.

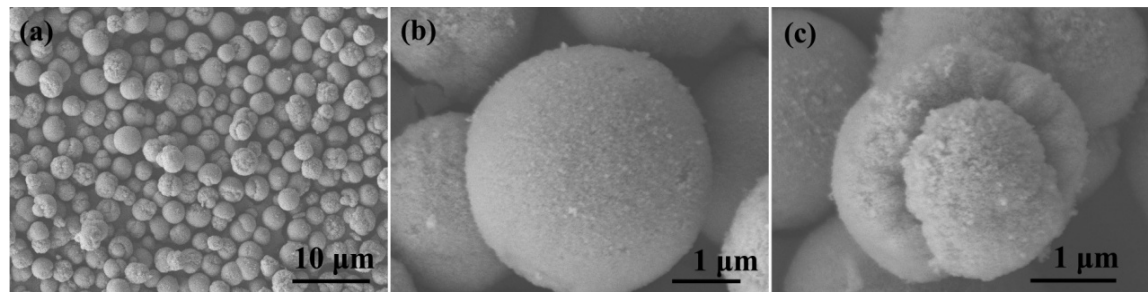


Fig. S9 FESEM image of the $\text{Mn}_{0.33}\text{Co}_{0.67}\text{CO}_3$ annealed for 10 h at 600 °C.

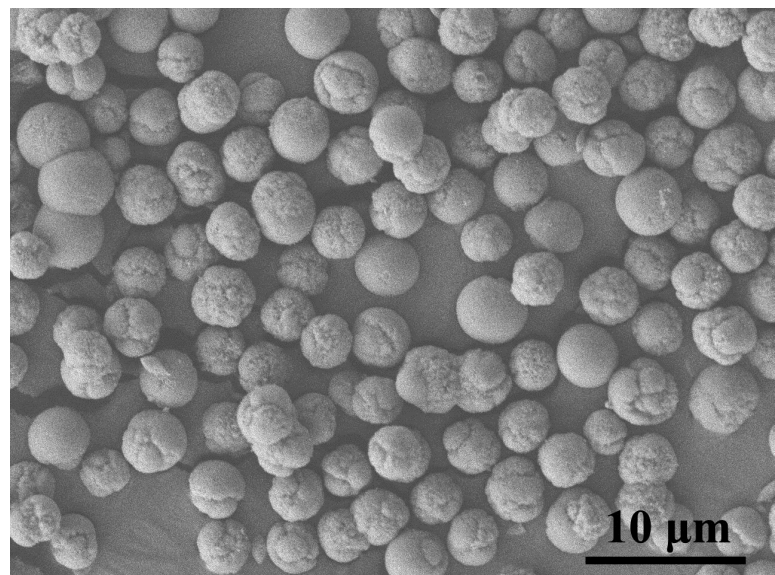


Fig. S10 FESEM image of the $\text{Mn}_{0.33}\text{Co}_{0.67}\text{CO}_3$ annealed for 12 h at 600 °C.

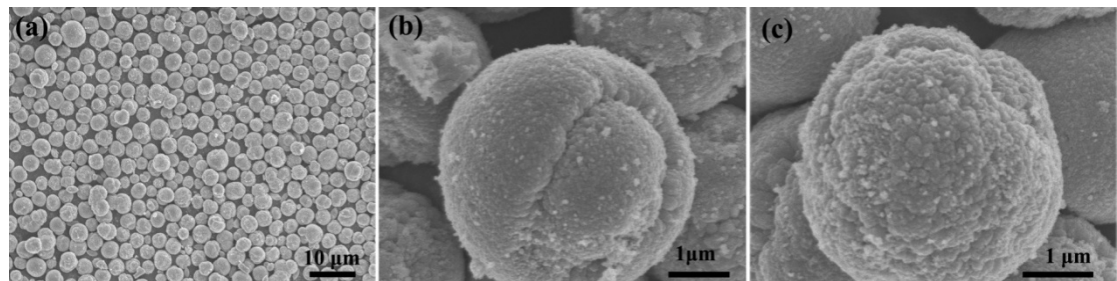


Fig. S11 FESEM image of the $\text{Mn}_{0.33}\text{Co}_{0.67}\text{CO}_3$ annealed for 16 h at 600 °C.

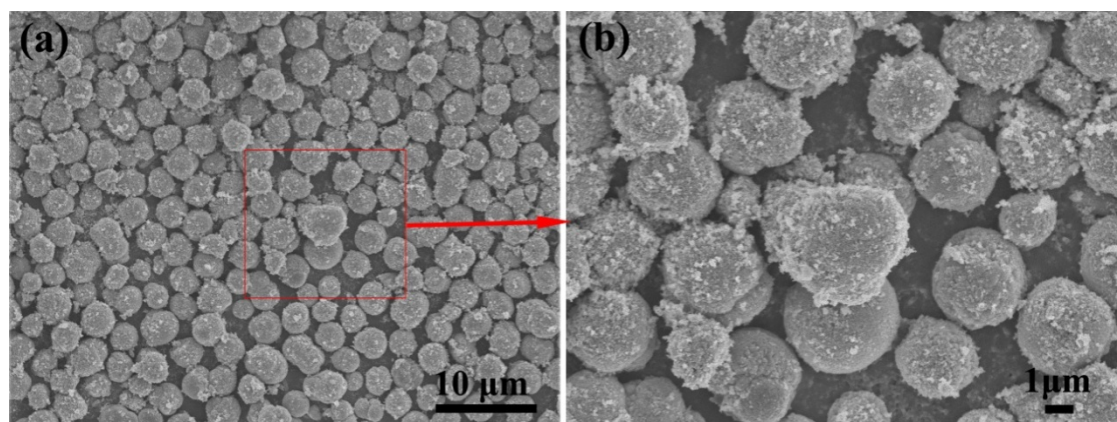


Fig. S12 FESEM image of the $\text{Mn}_{0.33}\text{Co}_{0.67}\text{CO}_3$ annealed for 24 h at 600 °C.

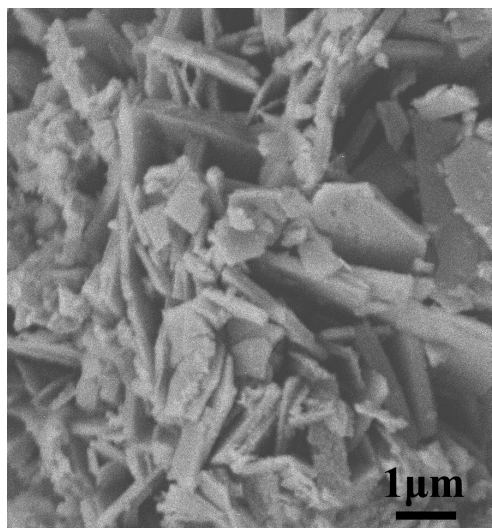


Fig. S13 FESEM image of the product in the absence of HMT in the reaction system.

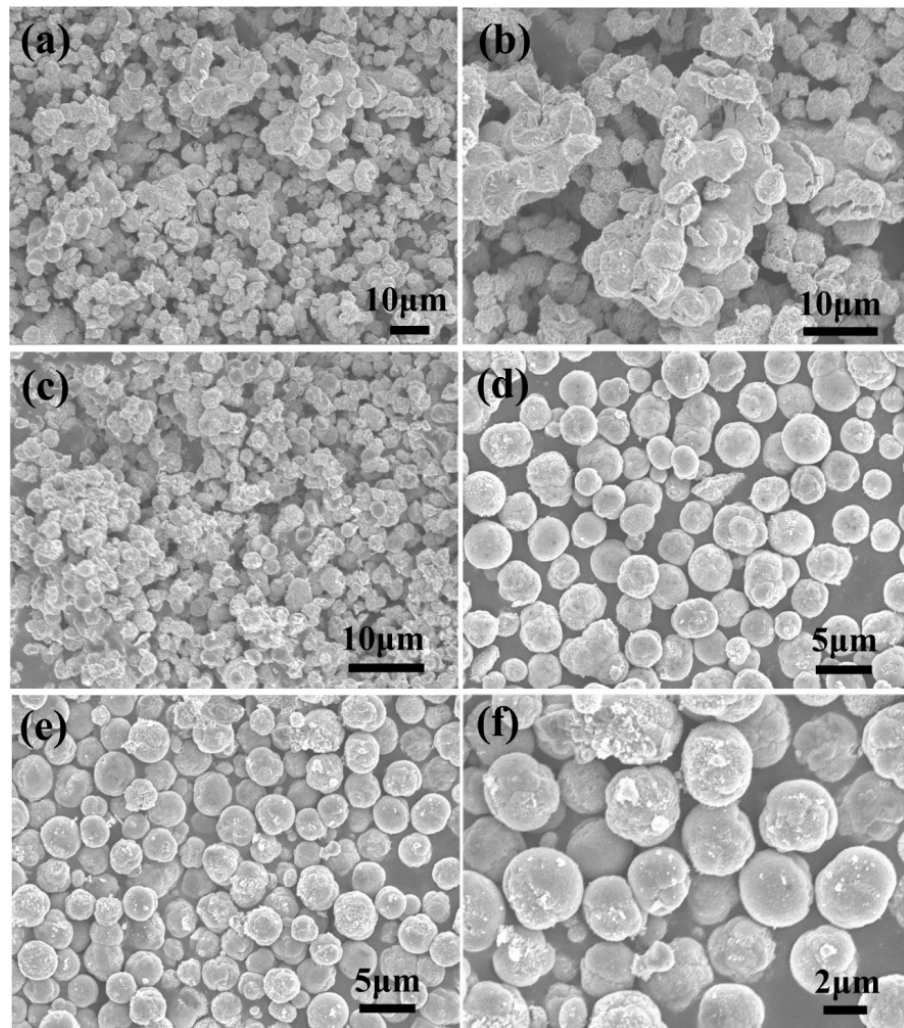
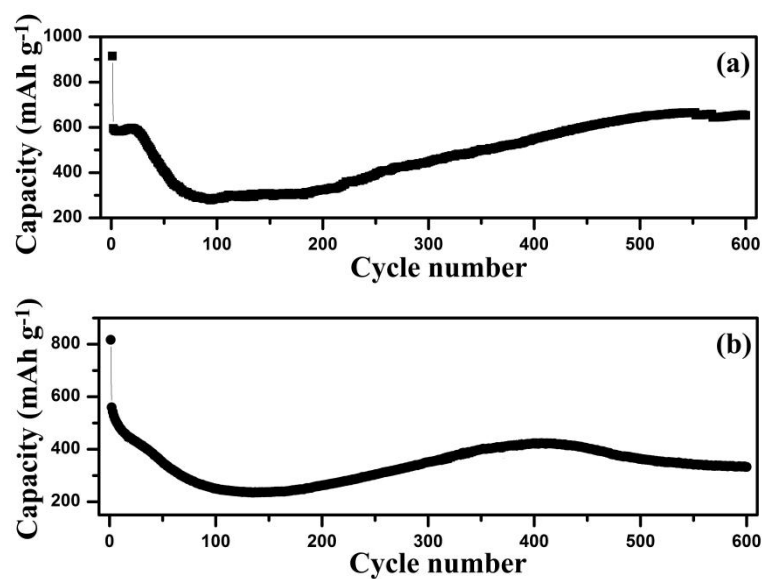


Fig. S14 FESEM images of the products obtained using different masses of HMT:
 (a,b) 0.1 g; (c) 0.5 g; (d) 3.0 g; (e,f) 5.0 g.



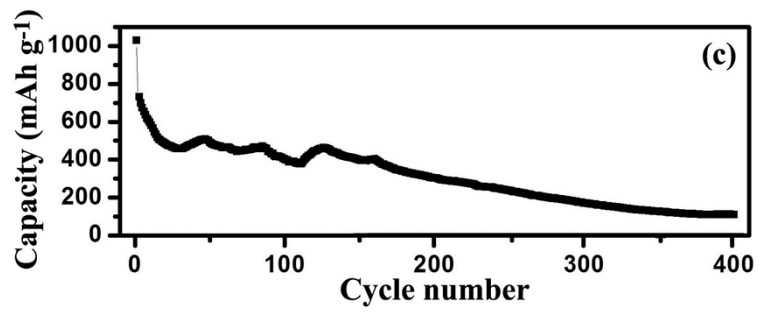


Fig. S15 Cycling performances of the yolk-shell structured (a) MnCo₂O₄ and (b) CoMn₂O₄ microspheres; (c) solid MnCo₂O₄ spheres at 1000 mAh g⁻¹.

Table S1 Morphology change processes of the mesoporous MnCo₂O₄ microspheres at different annealing time.

| Sample images | Fig. S2 | Fig. 3 | Fig. S6 | Fig. 5 and S7 |
|---------------|---|--|--|-------------------------|
| Conditions | 180 °C 12h | 600°C 2 h | 600°C 4h | 600°C 6h |
| Morphologies | MnCo-preserved $\text{Mn}_{0.33}\text{Co}_{0.66}\text{CO}_3$ | Mesoporous MnCo ₂ O ₄ microspheres | Transitional state to forming yolk-shell structure | Yolk-shell microspheres |
| Sample images | Fig. S8 | Fig. S9 | Fig. S10 | Fig. S11 |
| Conditions | 600°C 10h | 600°C 12h | 600°C 16h | 600°C 24h |
| Morphologies | Broken microspheres | Broken microspheres | Yolk and shell merge together gradually | Solid microspheres |

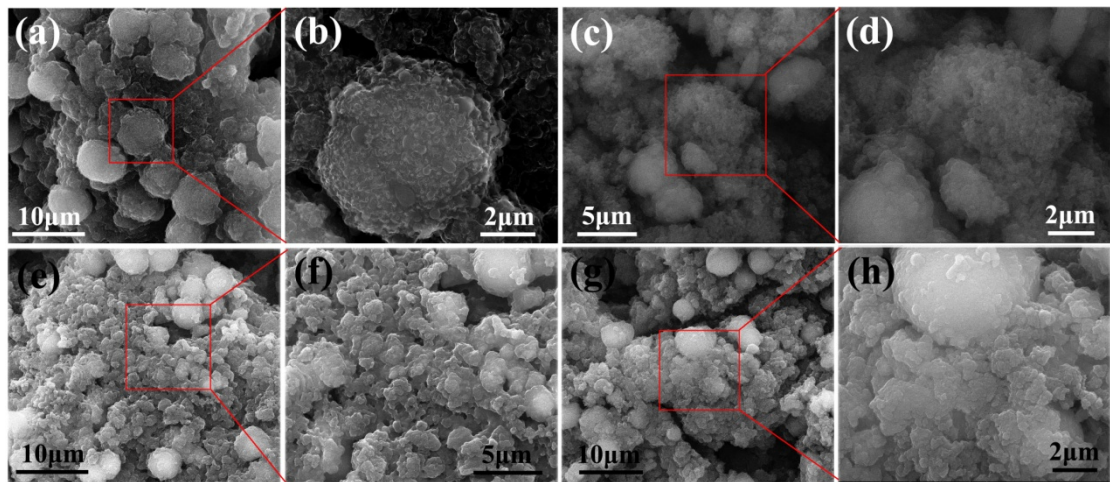


Fig. S16 FESEM images of the porous MnCo₂O₄ and CoMn₂O₄ microspheres after cycles: (a, b) MnCo₂O₄ after 200 cycles; (c, d) CoMn₂O₄ after 200 cycles; (e, f) MnCo₂O₄ after 1000 cycles; (g, h) CoMn₂O₄ after 1000 cycles.

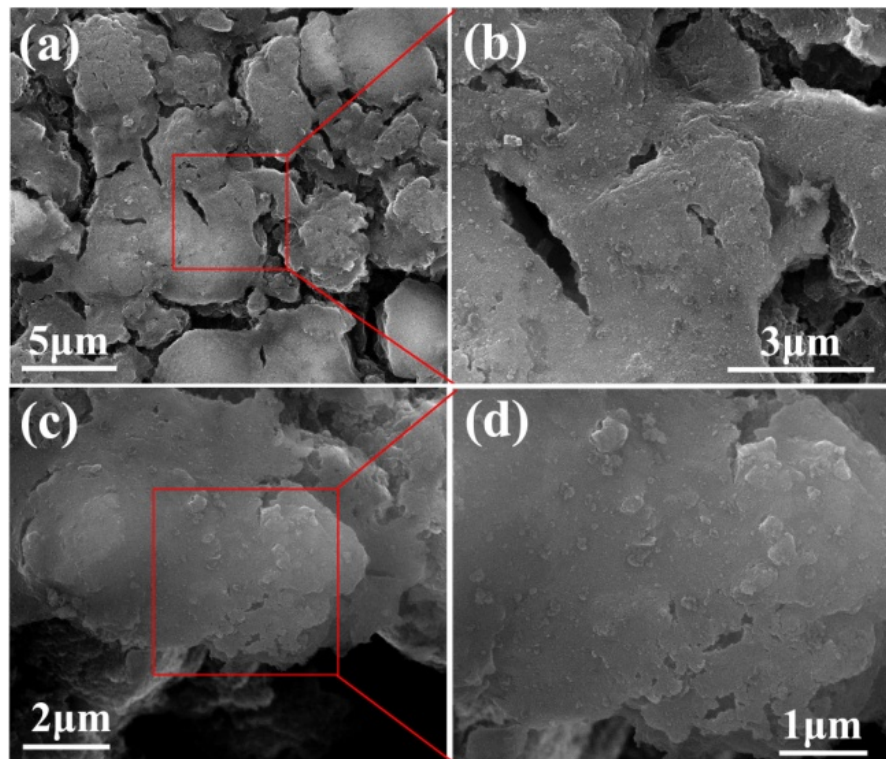


Fig. S17 SEI investigations of the porous (a, b) MnCo₂O₄ and (c, d) CoMn₂O₄ microspheres after 1000 cycles.

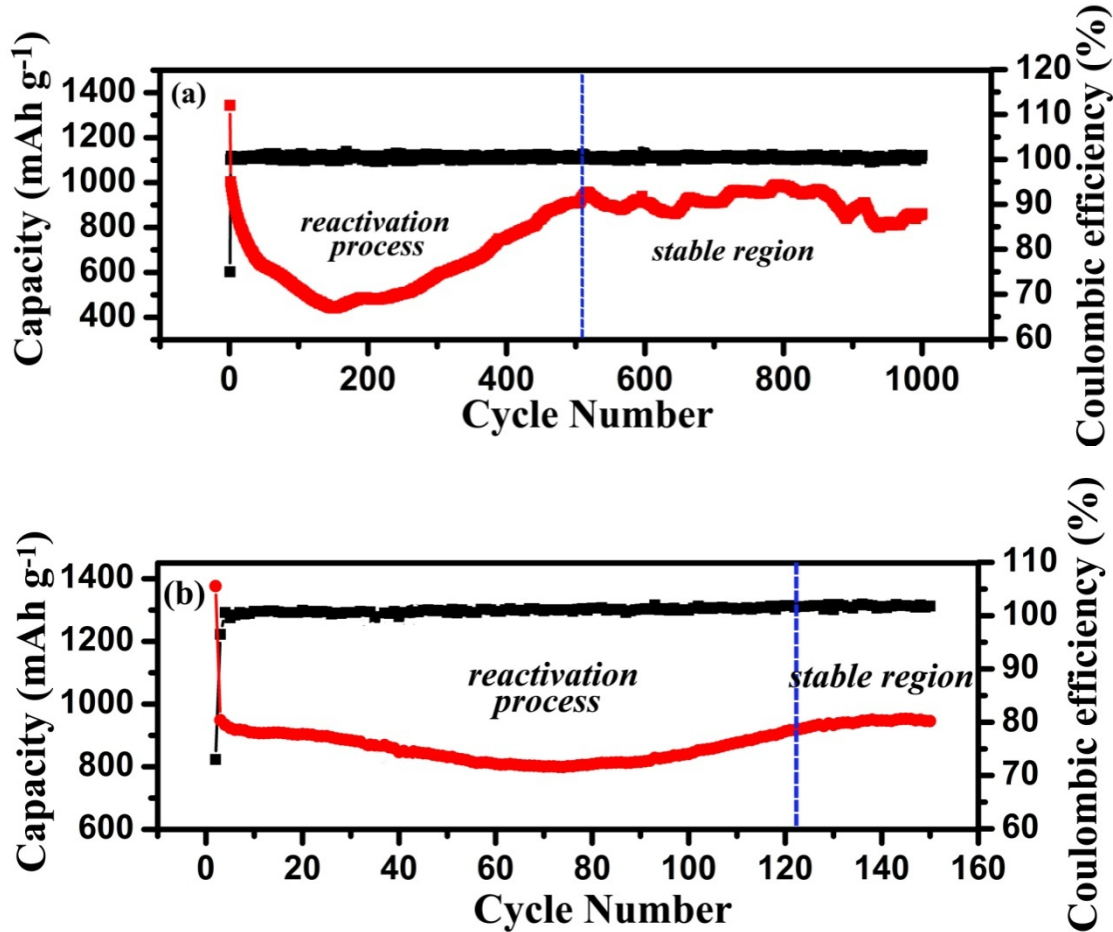


Fig. S18 Cycling performance of the mesoporous MnCo₂O₄ and CoMn₂O₄ microspheres electrode at a current density of 200 mA g⁻¹.

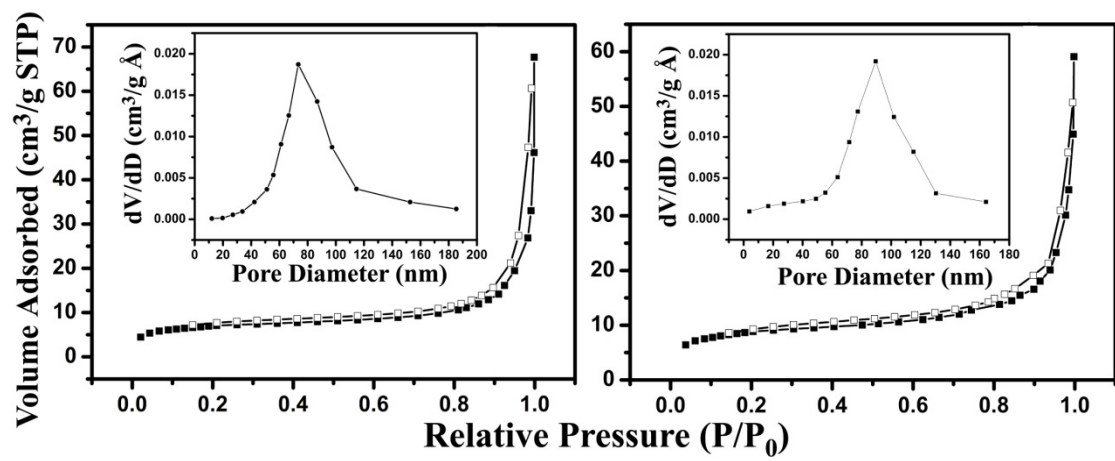


Fig. S19 N₂ adsorption/desorption isotherm and the corresponding pore size distribution of mesoporous MnCo₂O₄ and CoMn₂O₄ microspheres.

Table S2 Comparison of the cycling performance of MnCo₂O₄ and CoMn₂O₄ between our work and previous reports.

| Samples | Current density (mA g ⁻¹) | Cycle number | Reversible capacity (mAh g ⁻¹) | Ref. |
|---|--|--------------|---|-----------|
| MnCo ₂ O ₄ nanowire | 200 | 50 | 800 | 1 |
| MnCo ₂ O ₄ microsphere | 200 | 25 | 722 | 2 |
| MnCo ₂ O ₄ submicrosphere | 400 | 100 | 670 | 3 |
| MnCo ₂ O ₄ quasi-hollow sphere | 200 | 25 | 755 | 4 |
| CoMn ₂ O ₄ quasi-hollow sphere | 200 | 25 | 706 | 4 |
| MnCo ₂ O ₄ bulks or powders | 681 | 50 | 400 | 5 |
| CoMn ₂ O ₄ bulks or powders | 691 | 50 | 400 | 5 |
| CoMn ₂ O ₄ hollow microsphere | 200 | 50 | 624 | 6 |
| Mn _{1.5} Co _{1.5} O ₄ core-shell microsphere | 400 | 300 | 618 | 7 |
| CoMn ₂ O ₄ powder | 80 | 50 | 330 | 8 |
| Mesoporous MnCo ₂ O ₄ microsphere | 1000 | 1000 | 740 | This work |
| Mesoporous CoMn ₂ O ₄ microsphere | 1000 | 1000 | 420 | This work |

- [1] S. G. Mohamed, T. F. Hung, C. J. Chen, C. K. Chen, S. F. Hu, R. S. Liu, *RSC Adv.*, **2014**, 4, 17230.
- [2] C. C. Fu, G. S. Li, D. Luo, X. S. Huang, J. Zheng, L. P. Li, *ACS Appl. Mater. Interfaces*, **2014**, 6, 2439.
- [3] J. F. Li, J. Z. Wang, X. Liang, Z. J. Zhang, H. K. Liu, Y. T. Qian, *ACS Appl. Mater. Interfaces*, **2014**, 6, 24.
- [4] J. F. Li, S. L. Xiong, X. W. Li, Y. T. Qian, *Nanoscale*, **2013**, 5, 2045.
- [5] P. Lavala, J. L. Tirado, T. vidal-Abarca, *Electrochim. Acta*, **2007**, 52, 7986.
- [6] L. Zhou, D. Y. Zhao, X. W. Lou, *Adv. Mater.*, **2012**, 24, 745.
- [7] J. F. Li, S. L. Xiong, X. W. Li, Y. T. Qian, *J. Mater. Chem.*, **2012**, 22, 23254.
- [8] F. M. Courtel, H. Duncan, Y. Abu-Lebdeh, I. J. Davidson, *J. Mater. Chem.*, **2011**, 21, 10206.